HAL
open science

Radiation imaging with glass Micromegas

F.M. Brunbauer, D. Desforge, E. Ferrer-Ribas, F.J. Iguaz, B. Mehl, R. de Oliveira, E. Oliveri, T. Papaevangelou, O. Pizzirusso, E.C. Pollacco, et al.

To cite this version:

F.M. Brunbauer, D. Desforge, E. Ferrer-Ribas, F.J. Iguaz, B. Mehl, et al.. Radiation imaging with glass Micromegas. Nuclear Instruments and Methods in Physics Research Section A: Accelerators, Spectrometers, Detectors and Associated Equipment, 2020, 955, pp.163320. 10.1016/j.nima.2019.163320 . hal-02458765

HAL Id: hal-02458765

https://hal.science/hal-02458765v1

Submitted on 21 Jul 2022

HAL is a multi-disciplinary open access archive for the deposit and dissemination of scientific research documents, whether they are published or not. The documents may come from teaching and research institutions in France or abroad, or from public or private research centers.

L'archive ouverte pluridisciplinaire **HAL**, est destinée au dépôt et à la diffusion de documents scientifiques de niveau recherche, publiés ou non, émanant des établissements d'enseignement et de recherche français ou étrangers, des laboratoires publics ou privés.

Distributed under a Creative Commons Attribution - NonCommercial 4.0 International License

Version of Record: https://www.sciencedirect.com/science/article/pii/S0168900219315591
Manuscript_8490e8ad12053a2c6b36698d66de8ad0

Radiation imaging with glass Micromegas

F.M. Brunbauer[a], D. Desforge[b], E. Ferrer-Ribas[b], F.J. Iguaz[b], B. Mehl[a], R. De Oliveira[a], E. Oliveri[a], T. Papaevangelou[b], O. Pizzirusso[a], E.C. Pollacco[b,*], F. Resnati[a], L. Ropelewski[a], L. Segui[b], M. van Stenis[a]

[a] *European Organization for Nuclear Research (CERN), CH-1211 Geneve 23, Switzerland*
[b] *IRFU, CEA, Université Paris-Saclay, F-91191 Gif-sur-Yvette, France*

Abstract

Optically recording scintillation light emitted by MicroPattern Gaseous Detectors (MPGDs) with imaging sensors is a versatile and performant readout modality taking advantage of modern high granularity imaging sensors. To allow scintillation light readout of a detector based on MicroMesh Gaseous Structure (Micromegas) technology, we have integrated a Micromegas on a glass substrate with a transparent anode. In addition to optical detection of scintillation light emitted during electron avalanche multiplication between the micromesh and the anode, this setup also achieves a good energy resolution. A glass Micromegas detector was operated in an Ar/CF_4 gas mixture and showed a response comparable to conventional Micromegas detectors. The spectrum of the emitted scintillation light was recorded and shown to be equivalent to the one obtained with other gaseous detectors in the same gas mixture. Optically read out images were recorded with CCD cameras and integrated X-ray radiographic imaging with good spatial resolution was demonstrated. A spatial resolution of 440 µm (10% MTF) was found. Single X-ray photon detection with a high-sensitivity camera was achieved, which potentially permits energy-resolved X-ray fluorescence imaging.

Keywords: radiation imaging, optical readout, MPGD, Micromegas, glass Micromegas, scintillation, ITO

*Corresponding author
Email address: emmanuel.pollacco@cea.fr (E.C. Pollacco)

© 2019 published by Elsevier. This manuscript is made available under the CC BY NC user license
https://creativecommons.org/licenses/by-nc/4.0/

1. Introduction

Optical readout of MicroPattern Gaseous Detectors (MPGDs) takes advantage of combining the high gain factors achievable by MPGD technologies with the high granularity pixel readout permitted by modern imaging sensors. This allows for the realisation of radiation detectors with spatial resolution and sensitivity to a wide range of radiation ranging from Minimum Ionising Particles (MIPs) to low-energy X-rays, as well as highly ionising radiation such as alpha particles. Detector concepts based on optically read out MPGD-based detectors have been previously developed for applications such as radiation imaging [1, 2], 3D track reconstruction in optically read out Time Projection Chambers (TPCs) [3, 4] or dose imaging in hadron therapy [5, 6]. Previous MPGD-based detector concepts employing optical readout with imaging sensors were predominantly based on Gaseous Electron Multipliers (GEMs), a variety of MPGDs consisting of perforated multi-layer foils. This geometry makes GEMs well-suited for optical readout as scintillation light emitted during electron avalanche multiplication can be easily recorded by a camera placed behind the detector. In contrast, most other MPGD technologies are integrated on substrates such as Printed Circuit Boards (PCBs) which are opaque and thus inhibit scintillation light recording. This is also true for MicroMesh Gaseous Structures (Micromegas), which employ a micro-mesh supported by insulating pillars to create a uniform amplification region with an electric field strength sufficient for electron avalanche amplification between the micro-mesh and an anode [7]. However, Micromegas are typically integrated on PCBs, which has previously inhibited the optical readout of such detectors.

We have developed a Micromegas detector on a glass substrate with a transparent anode made of Indium Tin Oxide (ITO) to enable the optical readout of Micromegas-based detectors. Thus it is possible to take advantage of the superior energy resolution reached by this MPGD technology as well as profit from the high spatial resolution and intuitive 2D imaging capabilities associated

with optical readout with state-of-the-art imaging sensors.

This enables the readout of secondary scintillation light emitted during electron avalanche multiplication in the amplification gap between the micro-mesh and the anode. As with the optical readout of GEM-based detectors, the glass Micromegas were operated in an Ar+CF_4 gas mixture. Gas mixtures containing CF_4 feature wide scintillation light emission bands in the ultraviolet (UV) and visible (VIS) wavelength ranges [8], which are compatible with the wavelength-dependent quantum efficiency (QE) of common CCD and CMOS imaging sensors. Optical readout of GEM-based detectors operated in Ar+CF_4 gas mixtures has been reported and used for X-ray radiography [1, 2] as well as 3D track reconstruction [3, 4].

Optically transparent ITO anodes permitting scintillation light readout have previously been used to record charge spectra from a glass GEM detector [9] as well as for track reconstruction in an optically read out TPC [10]. In addition to featuring high optical transparency, good charge resolution was achieved by using an ITO layer on a glass substrate as anode.

2. Experimental setup of the glass Micromegas detector

The readout (Fig. 1, left) is a $6 \times 6\,\mathrm{cm}^2$ bulk Micromegas [11] built on a 1.1 mm thick Borosilicate glass support with an ITO single anode and an amplification gap of 128 µm, i.e., the distance between the anode and the mesh wires. The anode, built on the glass support, is a 45 nm thick ITO-layer with a sheet resistivity of $15\,\Omega/\square$ and an optical transparency of more than 80%. The mesh is a calendered squared-pattern woven stainless-steel one with 18 µm diameter wires, a hole aperture of 45 µm and a hole pitch of 63 µm. A microscopic image of the mesh is shown in Fig. 1 (right). The amplification gap is defined by 500 µm diameter pillars, arranged in square pattern and with a pitch of 6 mm. The mesh was stressed at a tension of 14 N/cm and laminated onto the glass at the Micro-Pattern Technologies (MPT) workshop at CERN. Electrical contact with the mesh and anode was achieved using silver-loaded adhesive.

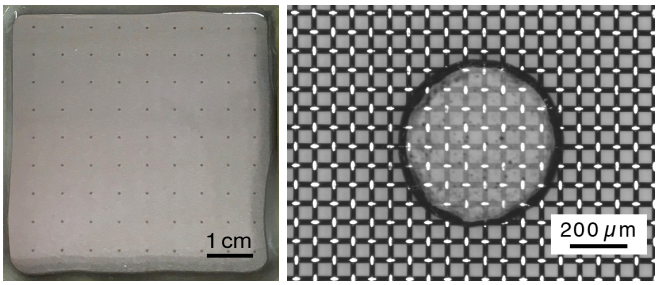

Figure 1: Left: The Micromegas detector prototype, composed of a woven stainless-steel mesh and an ITO coating ($15\,\Omega/\square$) for the anode on 1.1 mm thick glass with cylindrical pillars set in a square pattern. Right: Microscopic image of the squared-pattern woven stainless-steel mesh and one pillar.

The glass Micromegas was mounted in a gas volume with the glass substrate acting as a window as shown in Fig. 2. A single GEM mounted 2 mm above the glass Micromegas could act either as a cathode or as a pre-amplification stage. The drift volume was defined by a cathode composed of a polyimide foil coated with Cu, which was mounted 3 mm above the GEM foil. The detector was operated in an Ar+20%CF_4 gas mixture at atmospheric pressure in open gas flow mode at 5 l/h.

The glass Micromegas detector was optically read out with a low-noise 6 megapixel CCD camera (QImaging Retiga R6) located outside of the gas volume to demonstrate radiation imaging capabilities. The camera was placed at a distance of approximately 20 cm from the detector and a 17 mm focal length lens with an aperture of f/0.95 was used to focus scintillation light emitted in the detector onto the imaging sensor. The camera featured a $12.5 \times 10\,\mathrm{mm}^2$ imaging sensor with $4.54 \times 4.54\,\mu\mathrm{m}^2$ pixels. This setup resulted in a magnification factor of approximately 10.

The detector was operated in a stable condition at voltages of up to 600 V corresponding to an amplification field of 47 kV/cm. No discharges were observed during several hours of operation.

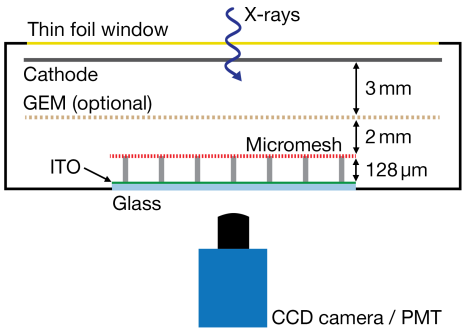

Figure 2: The glass Micromegas detector was mounted in a gas volume with a thin foil radiation window. The glass substrate was used as a window to read out scintillation light with a CCD camera located outside of the gas volume. The drift field was determined with a thin foil cathode and in some tests a GEM was used as pre-amplification structure. Schematic not drawn to scale.

3. Detector performance

The energy resolution achievable with optical readout of the prototype detector was measured and compared to the one obtained from the conventional electronic readout of charge signals in the same operational conditions. Energy spectra of an ^{55}Fe source were acquired by recording electrical signals at the anode of the detector using standard electronics. Simultaneously, scintillation light signals were acquired with a two-inch diameter PhotoMultiplier Tube (PMT, Hamamatsu R375) placed outside of the gas volume in direct contact with the glass substrate of the Micromegas detector. The experimental setup closely resembles the one shown in Fig. 2 with the PMT replacing the camera. The PMT was operated at a voltage of 1000 V yielding a gain of 2×10^5. The radiation source placed in front of the detector was collimated to result in a circular irradiated area with a diameter of approximately 5 mm. Collimation of the source was necessary to record energy spectra of the ^{55}Fe displaying both the full energy peak as well as the Ar escape peak. When using an uncollimated source, the varying geometric acceptance for detection of scintillation light emitted across the active area resulted in energy spectra, which did not display clearly separated peaks.

The energy spectra at a gain of 2000 obtained with electronic and optical readout are compared in Fig. 3. An energy resolution of 26 % FWHM was achieved when electronically reading out anode signals while a value of 24 % FWHM was obtained from scintillation light signals recorded with a PMT. The quoted resolution was obtained by fitting the sum of two gaussian functions, corresponding to the K_α (5.89 keV, 24.9 % intensity) and K_β (6.49 keV, 3.4 % intensity) emission lines of the ^{55}Fe source [12], to the energy range close to 6 keV. The similar energy resolution values for electronic and optical readout confirm that optically recorded signals can be used to determine deposited energy. This was previously shown for GEM-based detectors and a match between electronic and optical energy resolution was also reported [9, 1].

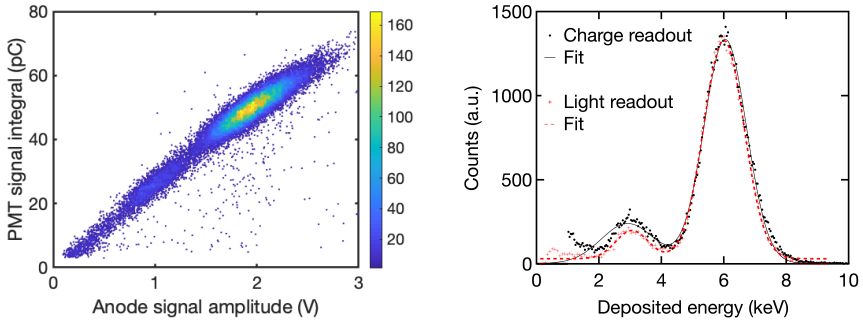

Figure 3: Energy spectra recorded under irradiation with ^{55}Fe source. Left: Correlation of anode signal amplitudes and PMT signal integrals. Right: An energy resolution of 26 % FWHM was achieved with electronic readout of anode signals and 24 % FWHM was obtained from scintillation light signals.

4. Scintillation spectrum and light yield

The spectrum of the secondary scintillation light emitted by the glass Micromegas detector operated in an Ar+20%CF_4 gas mixture was measured and compared to the spectrum of scintillation light emitted by a GEM-based detector [8] as shown in Fig. 4.

To record scintillation light emission spectra, a 5 mm diameter collimating

lens was placed outside of the gas volume directly below the detector in contact with the glass substrate on which the Micromegas was integrated. The collected light was guided by a 600 µm diameter multi-mode optical fibre to a CCD-based UV-VIS spectrometer (Ocean Optics FLAME-S-UV-VIS-ES) capable of recording spectra in a wavelength range from 200 nm to 800 nm. The spectrometry setup was calibrated for absolute irradiance with a deuterium-halogen absolute irradiance calibration light source. Multiple spectra were acquired with an integration time of 10 s each and then averaged. An averaged background spectrum recorded with the Micromegas detector switched off was subtracted from the acquired light spectra. To achieve sufficient scintillation light intensity for recording spectra, the detector was operated under intense X-ray irradiation from a Cu X-ray tube operated with an acceleration voltage of 20 kV and a tube current of 20 mA. The detector was operated with a drift field of 200 V/cm and an amplification field of 43 kV/cm resulting in an anode current slightly below 2 µA. The acquired spectrum of the scintillation light emission from the glass Micromegas detector prototype is shown in Figure 4.

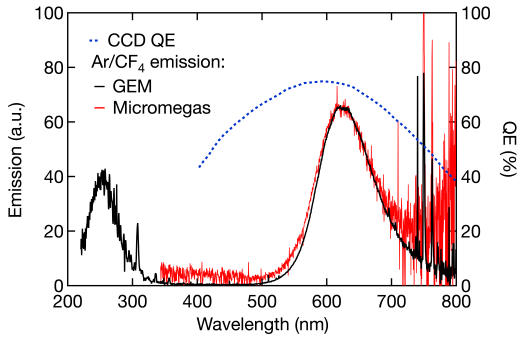

Figure 4: Scintillation light emission spectrum of glass Micromegas detector operated in an Ar+20%CF_4 gas mixture under X-ray irradiation. The QE of the CCD is compatible with the VIS emission band.

The recorded scintillation light emission spectrum agrees well with the emission spectra previously reported for GEM-based detectors operated in Ar-CF_4 gas mixtures [8]. An emission band in the VIS wavelength range centered around

630 nm as well as some sharp emission line in the near-infrared range could be identified. The wide VIS emission band is attributed to emission from CF_4 molecules, while the sharp emission lines are attributed to photons emitted as a result of transitions between different excited states of Ar atoms. Scintillation light emission in the UV range could not be recorded due to the opacity to UV light of the ITO layer and the glass substrate used as anode. Despite intense irradiation of the detector with an X-ray tube, the total emitted scintillation light intensity was low, which resulted in a significant noise level in the acquired spectra.

The secondary scintillation light yield of the glass Micromegas detector was measured to quantify the intensity of the emitted light. The light yield is defined as the ratio between the number of emitted scintillation photons and secondary electrons produced during electron avalanche multiplication.

Waveforms of PMT signals of individual events were acquired and integrated. The integrated intensity was divided by the integrated intensity corresponding to single photon events detected by the PMT to determine the number of recorded scintillation photons. The single photon response of the PMT was measured with a triggered LED operated at low voltage. Subsequently, the number of photons emitted during electron avalanche multiplication was calculated from the number of photons recorded by the PMT by taking into account correction factors for the geometric acceptance of the PMT and for the detection efficiency. The geometric acceptance correction factors were determined by counting the number of photons originally emitted in random directions from the active area of the detector which end up on the active area of the PMT. The detection efficiency correction factor was determined by multiplying the scintillation spectrum with the transmission of the ITO anode and the glass substrate and the quantum efficiency curve of the employed PMT. The light yield was measured for the configuration of the glass Micromegas detector operated with the GEM used as pre-amplification stage. For a 400 V potential difference across the GEM and an amplification field of 44 kV/cm in the glass Micromegas, a low light yield value of $0.12\,\mathrm{ph/e^-}$ was determined. This value is

significantly lower than previously obtained light yield values of approximately 0.5 ph/e$^-$ measured for triple-GEM detectors operated in an Ar+10%CF_4 gas mixture [8]. The discrepancy between the light yield values determined for the glass Micromegas detector and GEM-based detectors cannot be explained with the current measurements and is subject to further investigations.

5. X-ray radiography

The linearity of the response of the optically read out glass Micromegas detector was investigated by irradiating the detector with X-rays from an X-ray tube at varying beam intensities. The acquired images were obtained by recording the integrated light intensity with the camera in a fixed interval of time. The pixel value intensity in a center region of the acquired images as a function of the X-ray tube current is shown in Figure 5.

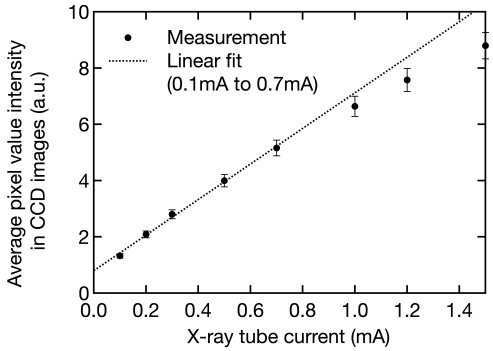

Figure 5: Linearity of CCD response. The averaged pixel value intensity increases almost linearly with the X-ray tube current for low X-ray tube currents and exhibits saturation.

The detector response remained linear at low X-ray fluxes but exhibits saturation at higher X-ray irradiation intensities. Therefore, the recorded pixel value intensity can be used to determine the intensity of the incident radiation at low X-ray fluxes.

The detector response across the active area was investigated by recording uniform exposure images of the detector under irradiation with an X-ray tube.

The X-ray tube was positioned approximately 65 cm from the detector to achieve an approximately flat irradiation field. A uniform exposure image is shown in Figure 6.

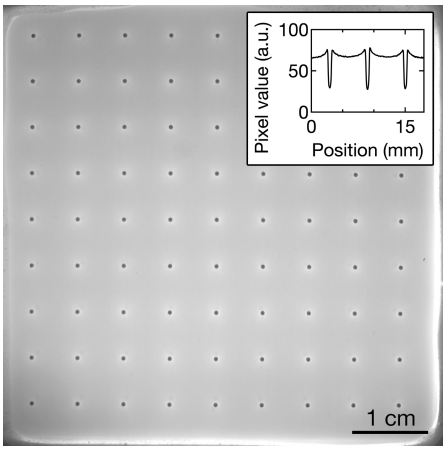

Figure 6: Uniform exposure image of glass Micromegas detector. Inset: Line profile of the pixel value intensity across pillars in the uniform exposure image.

The pillars are visible in uniform exposure images and correspond to dead regions in the active area of the detector. Around the pillars, increased pixel value intensities were observed. This is attributed to an increased number of electrons in these regions resulting from the modification of the electric field lines in the vicinity of the pillars [13]. However, we cannot exclude an optical effect where light is reflected off the pillars and this observation is therefore subject to further investigations and may eventually be resolved. A profile of the pixel value intensity across pillars in uniform exposure images is shown in the inset in Figure 6 and the pillars are clearly visible as dead regions in the profile. The brighter regions in the vicinity of the pillars are visible in the line profile of the pixel value intensity and appear to extend approximately 2 mm away from the pillars.

For X-ray radiography, the detector was irradiated with an X-ray tube with a Cu target operated at an acceleration voltage of 40 kV and the object under investigation was placed between the X-ray tube and the detector. A small

deceased animal was placed in front of the detector and a transmission X-ray radiograph was recorded by optically reading out scintillation light from the glass Micromegas detector. The detector was operated with an amplification field of 39 kV/cm corresponding to a gain of approximately 3×10^2. This resulted in a total current of 560 nA collected at the anode for an X-ray tube current of 1 mA. Multiple acquired images were averaged to achieve a high image quality. A background image was acquired without any X-ray irradiation and was subtracted from the acquired radiograph. To correct for the profile of the X-ray irradiation field, a "white" image was recorded without any object between the X-ray tube and the detector. Subsequently, the radiograph was divided by the "white" image to correct for the irradiation field profile. The resulting corrected radiograph is shown as the last image in Figure 7.

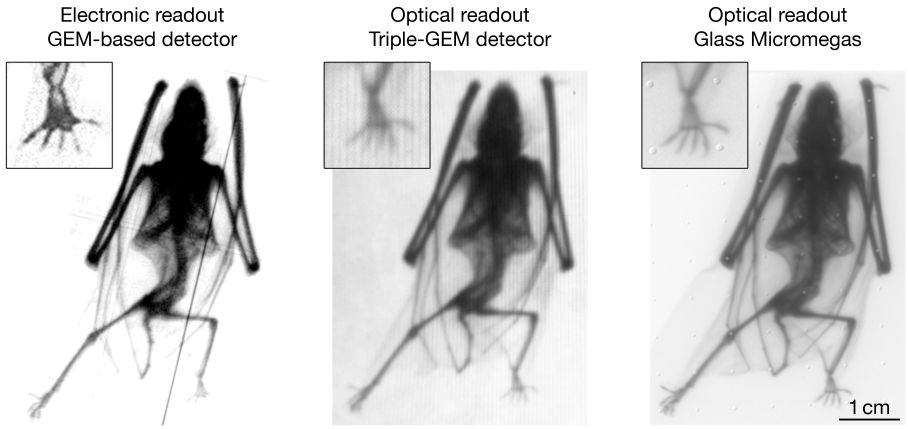

Figure 7: Comparison of transmission X-ray radiographies of a small bat with different detectors and readout modalities. The optical readout of the glass Micromegas detector achieves high resolution and intricate details are visible in the acquired images.

High resolution images could be acquired and the X-ray radiograph of the small bat shows internal bone structures as well as small features. The use of optically read out Micromegas enabled optical readout with higher resolution than in the case of triple-GEM-based detectors. This might be partly attributed to the localization of the light emission in the holes of GEM-based detectors as

shown in the inset in the central image in Figure 7 as well as in Figure 8. The glass Micromegas detector, in contrast, is an open system which features continuous light emission throughout the amplification gap since electron avalanches are not confined in the transversal direction. This results in images with a higher level of uniformity as shown in the inset in the right image in Figure 7. Images acquired with the GEM used as pre-amplification stage were qualitatively equivalent to images recorded with the Micromegas only.

The achievable spatial resolution in X-ray radiographs acquired by optical readout of the glass Micromegas detector was determined by imaging a 50 µm thick Pb foil with a line pair pattern. The test pattern was placed in direct contact with the cathode inside of the gas volume to minimise the distance to the active volume of the detector. The Modulation Transfer Function (MTF), defined as normalised contrast as a function of line pairs per millimetre (lp/mm), was measured and the lp/mm corresponding to a MTF of 10% was used to quantify the spatial resolution. For the glass Micromegas detector, a spatial resolution of 440 µm could be achieved. For an optically read out triple-GEM based detector operated at a higher gain, a spatial resolution of 890 µm was determined in a comparable experimental setup. The superior spatial resolution of the optically read out glass Micromegas detector may be partly attributed to the uniformity of the amplification structure in the case of the Micromegas as shown in Figure 8.

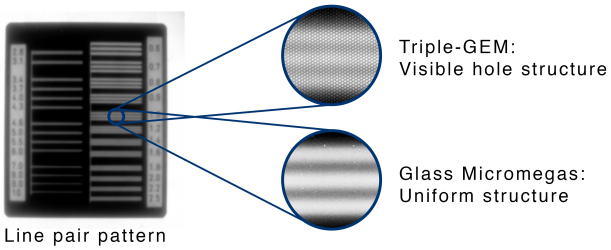

Figure 8: Comparison of optically recorded line pair pattern with GEM-based detector and glass Micromegas.

The enhanced energy resolution achievable with Micromegas detectors com-

pared to GEM-based detectors makes them an attractive candidate for energy-resolved imaging for applications such as X-ray fluorescence. To acquire energy-resolved 2D images with an optically read out gaseous radiation detector, short exposure images have to be acquired which display individual and distinguishable events. To investigate the applicability of the glass Micromegas detector for X-ray fluorescence, short exposure images under irradiation with an ^{55}Fe source were recorded. The recording of individual low-energy X-ray photon events requires a high detector gain and good sensitivity of the imaging sensors as the deposited energy of a single event is low. Therefore, the detector was operated with a GEM employed as pre-amplification stage with a potential difference of 400 V across the GEM. The glass Micromegas was operated with an amplification field of 47 kV/cm corresponding to a gain of approximately 6.7×10^3. In addition, a highly sensitive Electron Multiplying CCD (EMCCD, Hamamatsu ImagEM X2 C9100-23B) was used to record secondary scintillation light. This camera features a 0.25 megapixel sensor which employs impact ionisation to amplify signals by factors of up to 1200. This allowed the recording of short exposure images of individual low-energy X-ray photon events as shown in Figure 9.

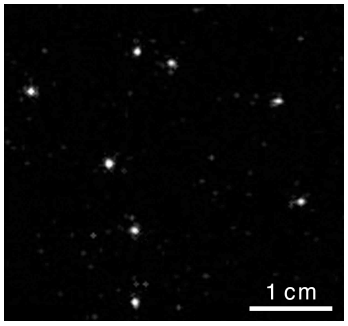

Figure 9: Short exposure image of individual low-energy X-ray photon events from an ^{55}Fe source acquired by an EMCCD camera.

In images recorded with short exposure times, individual X-ray photon events can be identified and the integrated pixel value intensities as well as the locations can be determined by a centre-of-gravity algorithm. The locations

and integrated intensities of a large number of events can be used for X-ray fluorescence imaging. For this imaging modality, the good energy resolution of the Micromegas detector along with the spatial resolution achieved by optical readout permit full-field energy-resolved imaging.

6. Conclusions

A Micromegas detector was integrated on a glass substrate with a transparent ITO layer as anode. Operating in an Ar+20%CF_4 gas mixture, secondary scintillation light emitted during electron multiplication in the amplification zone was recorded. The light emission spectrum was shown to be equivalent to the one of GEM-based detectors. A lower light yield normalised to the electronic gain compared to GEM-based detectors was measured.

The detector achieved a spatial resolution of 440 µm corresponding to a MTF of 10%. The superior spatial resolution compared to triple-GEM-based detectors is attributed to the uniformity of the amplification region and makes the glass Micromegas detector well-suited for imaging. Additionally, it achieves sufficient gain for recording individual low-energy X-ray photon events permitting energy-resolved imaging. Incorporating the glass Micromegas detector with ultra-fast imaging sensors and on-camera image processing, effective full-field X-ray fluorescence imaging might be realised. Recording and processing images at rates of several kHz and extracting tens of events from each frame may be used to rapidly assembly energy-resolved images.

The demonstrated possibility to integrate a Micromegas detector on a glass substrate enables the combination of this MPGD technology with optical readout. Thus, it can be used to benefit from the good energy resolution of Micromegas and the high granularity of imaging sensors.

Acknowledgements

We acknowledge the support of C. Bault (CERN) in constructing the experimental setup used for optical readout of the Micromegas detector. F.J. Iguaz ac-

knowledges the support from the Enhanced Eurotalents program (PCOFUND-GA-2013-600382).

References

[1] F. M. Brunbauer, M. Lupberger, E. Oliveri, F. Resnati, L. Ropelewski, C. Streli, P. Thuiner, M. Van Stenis, Radiation imaging with optically read out GEM-based detectors, JINST 13 (02) (2018) T02006. doi:10.1088/1748-0221/13/02/T02006.

[2] T. Fujiwara, Y. Mitsuya, T. Fushie, K. Murata, A. Kawamura, A. Koishikawa, H. Toyokawa, H. Takahashi, Gas scintillation glass GEM detector for high-resolution X-ray imaging and CT, Nucl. Instruments Methods Phys. Res. Sect. A 850 (January) (2017) 7–11. doi:10.1016/j.nima.2017.01.013.
URL http://dx.doi.org/10.1016/j.nima.2017.01.013http://linkinghub.elsevier.com/retrieve/pii/S016890021730013X

[3] L. Margato, F. Fraga, S. Fetal, M. Fraga, E. Balau, A. Blanco, R. F. Marques, A. Policarpo, Performance of an optical readout GEM-based TPC, Nucl. Instruments Methods Phys. Res. Sect. A 535 (1-2) (2004) 231–235. doi:10.1016/j.nima.2004.07.126.

[4] F. M. Brunbauer, G. Galgczi, D. Gonzalez Diaz, E. Oliveri, F. Resnati, L. Ropelewski, C. Streli, P. Thuiner, M. van Stenis, Live event reconstruction in an optically read out GEM-based TPC, Nucl. Instrum. Meth. A886 (2018) 24–29. doi:10.1016/j.nima.2017.12.077.

[5] E. Seravalli, M. de Boer, F. Geurink, J. Huizenga, R. Kreuger, J. M. Schippers, C. W. E. van Eijk, B. Voss, A scintillating gas detector for 2D dose measurements in clinical carbon beams, Phys. Med. Biol. 53 (17) (2008) 4651–4665. doi:10.1088/0031-9155/53/17/013.

[6] A. Klyachko, V. Moskvin, D. Nichiporov, K. Solberg, A GEM-based dose imaging detector with optical readout for proton radiotherapy, Nucl. Instruments Methods Phys. Res. Sect. A 694 (2012) 271–279. doi:10.1016/j.nima.2012.08.049.

[7] Y. Giomataris, P. Rebourgeard, J. P. Robert, G. Charpak, MICROMEGAS: A High granularity position sensitive gaseous detector for high particle flux environments, Nucl. Instrum. Meth. A376 (1996) 29–35. doi:10.1016/0168-9002(96)00175-1.

[8] M. M. F. R. Fraga, F. A. F. Fraga, S. T. G. Fetal, L. M. S. Margato, R. Ferreira-Marques, A. J. P. L. Policarpo, The GEM scintillation in He CF-4, Ar CF-4, Ar TEA and Xe TEA mixtures, Nucl. Instrum. Meth. A504 (2003) 88–92. doi:10.1016/S0168-9002(03)00758-7.

[9] T. Fujiwara, Y. Mitsuya, T. Yanagida, T. Saito, H. Toyokawa, H. Takahashi, High-photon-yield scintillation detector with Ar/CF 4 and glass gas electron multiplier, Jpn. J. Appl. Phys. 55 (10) (2016) 106401. doi:10.7567/JJAP.55.106401.
URL http://stacks.iop.org/1347-4065/55/i=10/a=106401?key=crossref.06ddd4ef4ef46b01583560ee0b4075f9

[10] F. M. Brunbauer, F. Garcia, T. Korkalainen, A. Lugstein, M. Lupberger, E. Oliveri, D. Pfeiffer, L. Ropelewski, P. Thuiner, M. Schinnerl, Combined optical and electronic readout for event reconstruction in a GEM-based TPC, IEEE Trans. Nucl. Sci. 65 (3) (2018) 913–918. doi:10.1109/TNS.2018.2800775.

[11] I. Giomataris, et al., Micromegas in a bulk, Nucl. Instrum. Meth. A560 (2006) 405–408. doi:10.1016/j.nima.2005.12.222.

[12] U. Schötzig, H. Schrader, Halbwertszeiten und photonenemissionswahrscheinlichkeiten von häufig verwendeten radionukliden, Tech. Rep. PTB-Ra-16/5, Physikalisch-Technische Bundesanstalt (1998).

[13] O. Sidiropoulou, Characterization of the ATLAS-type Micromegas Detectors, Ph.D. thesis, Julius-Maximilians-Universität Würzburg (2018). URL https://opus.bibliothek.uni-wuerzburg.de/frontdoor/index/index/docId/16732